Tetrasubstituted α-pyrone derivatives from the endophytic fungus, *Neurospora udagawae*

Allan Patrick G. Macabeo[a, b], Allaine Jean C. Cruz[a], Abolfazl Narmani[b, c], Mahdi Arzanlou[c], Asadollah Babai-Ahari[c], Luis Agustin E. Pilapil[a], Katherine Yasmin M. Garcia[a], Volker Huch[d] and Marc Stadler[b, *]

[a] *Laboratory for Organic Reactivity, Discovery and Synthesis (LORDS), Research Center for the Natural and Applied Sciences, University of Santo Tomas, Espana Blvd., 1015 Manila, Philippines*

[b] *Department of Microbial Drugs, Helmholtz Center for Infection Research (HZI), and German Center for Infection Research (DZIF), Partner Site Hannover/Braunschweig, Inhoffenstraße 7, 38124 Braunschweig, Germany*

[c] *Department of Plant Protection, Faculty of Agriculture, University of Tabriz, Tabriz, Iran*

[d] *Servicestelle Strukturanalyse Chemie, Universität des Saarlandes, 66041 Saarbrücken, Germany*

Abstract

Two new α-pyrone derivatives, udagawanones A (**1**) and B (**2**), along with the known compounds (*Z*)-4-hydroxy-3-(3-hydroxy-3-methylbut-1-en-1-yl)benzoic acid (**3**), isosclerone (**4**), *cyclo*-(*L*-Leu-*L*-Pro) (**5**), and *cyclo*-(*L*-Pro-*L*-Tyr) (**6**), were isolated from cultures of the endophyte *Neurospora udagawae.* Their structures were elucidated by extensive spectroscopic methods and single crystal X-ray diffraction. Both compounds feature oxidized functionalities at the C-2 position not previously observed in other tetrasubstituted α-pyrones from fungi. Compound **1** exhibited moderate antibacterial (vs. *Staphylococcus aureus*) and antifungal (vs. *Rhodoturula glutinis*) activities and cytotoxicity against KB3.1 cells.

Keywords: α-pyrones, endophytic fungi, antimicrobial, cytotoxic

1. Introduction

Exploration of unique biological niches for discovering new generations of antimicrobial and anti-cancer drugs, may provide solutions to combat drug-resistant microorganisms and cancer cells. For example, coprophilous fungi have proven to be promising source of secondary metabolites to combat pathogens and cancer cells which are becoming increasingly resistant to drugs and antibiotics (Helaly et al.,2018). Fungi exhibit different life styles, but it is difficult to define distinct boundaries to separate fungal life styles. Most of them show continuum lifestyle from biotrophy to necrotrophy and eventually saprotrophy (Bills et al., 2013; Bills and Gloer, 2016; Karwehl and Stadler, 2016). Coprophilous fungi are commonplace and ubiquitous organisms that exhibit saprotrophy life style (Bills et al., 2013; Bills and Gloer, 2016; Karwehl and Stadler, 2016). It has been proven that these fungi, like other filamentous fungi, have developed a variety of metabolic pathways necessary to produce secondary metabolites that can affect other organisms because they dwell in highly competitive and transient habitats (Bills et al., 2013; Bills and Gloer, 2016). Their enormous biodiversity, in addition to their ability to produce a variety of biologically active natural products has propelled a number of exploratory efforts on their rich secondary metabolism (Karwehl and Stadler, 2016). To date, only a small proportion of global fungal biodiversity has been studied for bioactive compounds, hence the study of new and hitherto untapped species may still yield a plethora of novel bioactive molecules (Zhao et al., 2010)

During a survey of endophytic fungi in August 2016, in the Kaleybar region, northwestern zone of Iran, healthy, 2 to 3-year-old shoots were obtained from the Oak trees (*Quercus macranthera,* family Fagaceae) from which, the fungus, *Neurospora udagawae*, was isolated and identified through morphological and molecular phylogenetic methods (Garcia et al., 2004). It is

generally accepted that *Gelasinospora* and *Neurospora* are synonymous genera and so far 49 species of *Neurospora* have been identified (Garcia et al., 2004). The fungus *N. udagawae* has been reported in Pakistan and Iran from soil and plant debris, respectively. In this study, this fungus was isolated as an endophyte for the first time. According to previously reported habitats of this fungus, contradictions may have been due to the ineffectiveness of fungal endophyte isolation methods (Garcia et al., 2004). Species of the genus *Neurospora* have previously led to the production of bioactive compounds such as *α*-pyrones, butenolides and furan-containing polyketides. These α-pyrone metabolites possess immunosuppresive effects against the proliferation of mouse spleen lymphocytes stimulated with Con A and lipopolysaccharide (Fujimoto et al., 1995; Fujimoto et al., 1998; Fujimoto et al., 1999; Fujimoto et al., 2006; Fujimoto, 2018). As part of our on-going exploration on the secondary metabolism of Iranian fungi (Narmani et al., 2018; Narmani et al., 2019), we hereby disclose the isolation and structure elucidation of two new tetrasubstituted *α*-pyrone derivatives, udagawanones A (**1**) and B (**2**), from, *N. udagawae* using spectroscopic methods, and their biological activities.

2. Results and discussion

The LC-MS-UV(DAD) profile of the EtOAc extract of *N. udagawae* cultures showed the presence of several conjugated derivatives, which exhibited characteristic UV maxima at approximately 220 and 300 nm reminiscent of pyrone and other aromatic metabolites. *N. udagawae* was grown in yeast-malt (pH 6.3) media (Kuephadungphan et al., 2019; Phukhamsakda et al., 2018), and extracts from its culture were fractionated and purified using reversed-phase C18 preparative HPLC. This work provided two new *α*-pyrone derivatives (**1** and **2**) along with four known fungal secondary metabolites. Herein, we report the isolation, structure elucidation, and biological activities of udagawanones A (**1**) and B (**2**) (Fig. 1).

Compound **1** was isolated as colorless crystals, and its molecular formula was determined as $C_{11}H_{14}O_4$ based on its sodiated molecular ion peak $[M + Na]^+$ at *m/z* 233.0782 by HRESIMS and through analysis of its ^1H and ^{13}C NMR spectroscopic data, suggesting an index of hydrogen deficiency of five. The UV maxima at approximately 222 and 336 nm suggested the presence of an *α*-pyrone substructure (Fujimoto et al., 1995; Fujimoto et al., 1998; Fujimoto et al., 1999; Chomcheon et al., 2009; Kim et al., 2018). The IR spectrum (KBr) suggested the presence of hydroxyl (3400 cm^{-1}), conjugated carboxyl ester (1670 cm^{-1}) and olefinic (1541 cm^{-1}) functional groups. The ^1H NMR spectrum of **1** showed two olefinic protons, two oxygenated methines, an oxygenated methylene, a methoxy signal, an exchangeable proton and two methyl signals. The ^1H, ^{13}C, and DEPT NMR data in conjunction with the HSQC spectroscopic data of **1** suggested the presence of eleven carbons, containing a carboxyl carbon, four non-protonated sp^2 carbons, two olefinic methine carbons, an oxymethylene carbon, a methoxy carbon, and two other methyl carbons (Table 1). The propenyl moiety corresponding to C-1′-C-2′-C-3′ was deduced from the COSY spectrum. The gross planar structure of **1** was elucidated by analyzing the 2D NMR data, including HMBC and ROESY (Fig. 2). The HMBC correlations of H_2-1″ to C-2, C-3 and C-4, OMe-4 to C-3, C-4and C-5, and H-2″ to C-4, C-5 and C-6 suggested the presence of a pyrone core structure. A primary alcohol was assigned by HMBC correlation from OH-1″ to C-1″. The HMBC correlations from H-1′ and H-2′ to C-6 established the connection of *α*-pyrone substructure to the propenyl chain. In addition, the ROESY correlations from H_2-1″ and H_3-2″ to OMe-4 and from H-1′ to H_3-2″ supported the position of the four substituents. The planar structure of **1** was elucidated as depicted and supported by X-ray experiments (Fig. 2) and thus, was identified as (*E*)-3-(hydroxymethyl)-4-methoxy-5-methyl-6-(prop-1-en-1-yl)-2*H*-pyran-2-one or udagawanone A.

Compound **2** was obtained as a colorless oil, and its molecular formula was established as $C_{10}H_{10}O_4$ by HRESIMS based on its protonated molecular ion peak at *m/z* 195.0840, and by analysis of its ^{1}H and ^{13}C NMR spectroscopic data pointing to an index of hydrogen deficiency of six. The IR spectrum (KBr) suggested the presence of hydroxyl (3341 cm^{-1}), aldehyde (1684 cm^{-1}), conjugated carboxyl ester (1651 cm^{-1}) and olefinic (1625 cm^{-1}) functional groups. The UV maxima and NMR data were very similar to those of **1** (Table 1), suggesting the same basic carbon skeleton. However, the exchangeable signal of OH-1′ (δ_H 3.05) and the methyl group in the OMe-4 moiety in **1** were not present in the ^{1}H NMR data of **2**. The oxymethylene signal of **1** at the C-1′ (δ_C 61.9) position was replaced by a carboxaldehyde signal (δ_H 9.94; δ_C 191.8) in the NMR spectrum of **2**. The structure of **2** was determined as shown in Figure 1, and was identified as (*E*)-4-hydroxy-5-methyl-2-oxo-6-(prop-1-en-1-yl)-2*H*-pyran-3-carbaldehyde, and was given the trivial name, udagawanone B (**2**).

Most fungi produce trisubstituted *α*-pyrone derivatives with typical substitutions at C–3 (or 5), C–4 (with a methoxy group) and C–6, while tetrasubstituted congeners have been observed exclusively in the genus *Neurospora*. Previous studies indicated the occurrence of highly oxidized tetrasubstituted *α*-pyrone derivatives from *N. heterospora*, *N. multiforis* and *N. longispora* where C–3 and C–5 are functionalized with either formyl or methylene hydroxyl groups (Fujimoto et al., 1995; Fujimoto et al., 1998; Fujimoto et al., 1999; Fujimoto et al., 2006; Fujimoto, 2018). Interestingly, both udagawanones A (**1**) and B (**2**) represent structures of the less oxidized congeners. In addition, compound **2** is also a first example of a non-methylated C–4 derivative.

Four known compounds were also isolated and purified from *N. udagawae*. These were identified as (*Z*)-4-hydroxy-3-(3-hydroxy-3-methylbut-1-en-1-yl)benzoic acid (**3**) (Zhao et al.,

2018), the tetralone derivative isosclerone (**4**) (Machida et al., 2005), *cyclo*-(*L*-Leu-*L*-Pro) (**5**) (Jayatilake et al., 1996), and *cyclo*-(*L*-Pro-*L*-Tyr) (**6**) (Jayatilake et al., 1996) by comparing their spectroscopic data (MS, ^{1}H and ^{13}C NMR) with literature values. Our study is the second report on the isolation of the meroterpenoid **3** being identified recently from a strain of the mycophilic, pleosporalean ascomyete *Montagnula donacina* that was associated with the edible mushroom *Craterellus odoratus* (Zhao et al., 2018).

Compounds **1** and B **2** also share structural similarities with the known α-pyrone derivatives dothideopyrones A−F isolated from the endophytic fungus Dothideomycetes spp. (Chomcheon et al., 2009; Kim et al., 2018), however, lacking a methyl substituent at C-5 and featuring an elaborate alkyl side chain at C-6. Previous reports showed these α-pyrones weak to inactive against cancer cell lines. Dothideopyrone F, however, showed moderate anti- inflammatory effects in LPS- stimulated BV2 microglial cell thus, validating previous biological studies on this class of α-pyrone natural products. Exploring the biological activity of **1** and **2**, udagawanone A (**1**) exhibited moderate anti-bacterial activity against *Staphylococcus aureus* and anti-fungal activity against *Rhodoturula glutinis* with MIC of 66 μg/mL using serial dilution antimicrobial assay methods (Cheng et al., 2019). In addition, both compounds showed moderate cytotoxic activities against KB3.1 (HeLa cells) (**1**: IC_{50} = 27 μg/mL; **2**: IC_{50} = 27 μg/mL) while displaying weak to insignificant cytotoxicity against human fibroblast cells (L929). Finally, weak enzyme inhibitory activities were observed for **1** and **2** against α-glucosidase and porcine lipase (IC_{50} = >100 μg/mL).

In conclusion, chemical investigation of the ethyl acetate extract of the broth culture of *N. udagawae* obtained from the Iranian *Quercus macranthera* led to the isolation and structure identification of two highly substituted α-pyrone congeners, udagawanones A (**1**) and B (**2**), and

four previously reported metabolites (**3**–**6**). The above fungus was identified by means of morphological studies and molecular phylogenetic methods. Although the isolated compounds were moderately active against fungi and mammalian cells, this is the first report describing metabolites from *N. udagawae.*

3. Experimental

3.1. General Experimental Procedures

UV spectra were recorded with a Shimadzu UV–vis spectrophotometer UV-2450. IR spectra (KBr) were obtained on a Shimadzu FTIR Prestige-21 spectrophotometer. NMR spectra were recorded on a Bruker 500 MHz Avance III spectrometer with a BBFO (plus) SmartProbe (^{1}H 500 MHz, ^{13}C 125 MHz), and Bruker 700 MHz Avance III. Chemical shifts are given in parts per million (ppm), and coupling constants in Hertz (Hz). Spectra were measured in $CDCl_3$ and methanol-d_4, and chemical shifts were referenced to the solvent signals (7.27 ppm for ^{1}H and 77.7 ppm for ^{13}C for $CDCl_3$; 3.31 and 4.87 ppm for ^{1}H and 49.1 ppm for ^{13}C for methanol-d_4). HPLC-DAD-MS analysis was performed using an amaZon speed ETD ion trap mass spectrometer (Bruker Daltonics) in positive and negative ionization modes. The mass spectrometer was coupled to a DIONEX UltiMate 3000 with a Diode Array Detector [column 2.1 × 50 mm, 1.7µm, C18 Acquity UPLC BEH (Waters), solvent A: H_2O + 0.1% formic acid; solvent B: acetonitrile (ACN) + 0.1% formic acid, gradient: 5% B for 0.5 min, increasing to 100% B in 20 min, maintaining isocratic conditions at 100% B for 10 min, flow = 0.6 mL/min, UV–vis detection 200–600 nm]. HR-ESI-MS spectra were recorded on a maXis ESI TOF mass spectrometer (Bruker Daltonics) [scan range m/z 100–2500, rate 2 Hz, capillary voltage 4500 V, dry temperature 200 °C], coupled to an Agilent 1200 series HPLC-UV system [column 2.1 × 50 mm, 1.7 µm, C18 Acquity uPLC BEH (Waters), solvent A: H_2O + 0.1% formic acid; solvent B:

ACN+0.1% formic acid, gradient: 5% B for 0.5 min, increasing to 100% B in 19.5 min, maintaining 100% B for 5 min, FR = 0.6 mL/min, UV–vis detection 200–600 nm]. The molecular formula were calculated including the isotopic pattern (Smart Formula algorithm). Preparative HPLC purification was performed at room temperature on an Agilent 1100 series preparative HPLC system [ChemStation software (Rev. B.04.03 SP1); binary pump system; column: Kinete×5u RP C18, dimensions 250×21.20mm; mobile phase: ACN + 0.05% trifluoroacetic acid (TFA) (Solvent B) and water + 0.05% TFA (Solvent A); flow rate 20 mL/min; diode-array UV detector; 226 fraction collector].

3.2 *Isolation and identification of endophytic fungus*

Quercus macranthera shoots (15-20 cm length) were surface-sterilized for 45-60 seconds in 70% ethanol, then sterilized in 3% sodium hypochlorite (NaClO) for 10 min and 30 seconds in 70% ethanol to rinsed sodium hypochlorite. Shoots were then dried on sterile tissue paper in a laminar flow hood. Small fragments were cut from the shoots and transferred on Malt Extract Agar (MEA) plate supplemented with 100 mg/L streptomycin sulphate and 100 mg/L ampicillin. Purification was performed using hyphal tip technique. On the basis of the ITS-rDNA phylogeny (Fig. S1) and morphological study (Fig. S2), the isolate was identified as *Neurospora udagawae*. Consensus sequence of ITS-rDNA of *N. udagawae* CCTU A145 was deposited in GenBank with accession number MK886745.

3.3 *Fermentation, extraction and isolation*

Pieces of a well-grown agar culture of *N. udagawae* were inoculated in a 500 mL Erlenmeyer flask containing 200 mL of YMG medium consisting of 1.0% malt extract, 0.4% glucose, and 0.4% yeast extract, pH 6.3 and incubated at 23 °C for 6 days. This 6-day-old seed culture was used to inoculate 25 x 200 mL other flasks (5 L) of the same medium composition.

The flasks were incubated at 23 °C under constant shaking at 140 rpm on a rotary shaker for 7 days. After separation from fungal mycelia by filtration, the supernatant was extracted with ethyl acetate. The combined ethyl acetate layer was dried over anhydrous sodium sulfate, filtered, and concentrated under reduced pressure to yield 515.1 mg of a reddish-brown extract.

The crude ethyl acetate extract (515.0 mg) was dissolved in methanol and purified by preparative HPLC using a gradient of 0 - 15% solvent B for 3 minutes, 15 - 100% B for 20 min, and 100% B for 10 min. The fractions were combined according to UV absorption at 220, 260, and 280 nm and concurrent HPLC-MS-UV (DAD) analyses. Compounds **1** (129.67 mg; t_R = 14.85 min), **2** (2.1 mg; t_R = 12.8 min), **3** (0.8 mg; t_R = 18.8 min), **4** (1.1 mg; t_R = 12.4 min), **5** (8.5 mg; t_R = 10.0 min) and **6** (1.2 mg; t_R = 6.76 min) were eluted.

Udagawanone A (**1**): White solid; UV (MeOH, *c* 0.25 mg/mL) λ_{max} (log ε) 336 (1.82), 222 (4.52) nm; HR-ESIMS *m/z* 233.0782 $[M + Na]^+$ (calcd for $C_{11}H_{14}O_4Na$, 233.0781); ^1H NMR ($CDCl_3$, 500 MHz) and ^{13}C NMR ($CDCl_3$, 125 MHz) data, see Table 1.

Udagawanone B (**2**): Colorless oil; UV (MeOH, *c* 0.25 mg/mL) λ_{max} (log ε) 291 (3.99), 337 (4.12), 221 (4.56) nm; HR-ESIMS *m/z* 195.0840 $[M + H]^+$ (calcd for $C_{10}H_{11}O_4$, 195.0859); ^1H NMR (MeOH-d_4, 700 MHz) and ^{13}C NMR (MeOH-d_4, 175 MHz) data, see Table 1.

*3.4 X-ray Crystallographic Analysis of Udagawanone A (**1**)*

Colorless crystals of **1** were obtained from a chloroform solution. The crystal of **1** was measured with a Bruker D8 Venture diffractometer with a microfocus tube, Cu Kα radiation (λ = 1.54178 Å). APEX3 was used for data collection, SAINT was used for cell refinement and data reduction, and SADABS was used for experimental absorption correction. The structure was solved by intrinsic phasing using SHELXT, while refinement was done by full-matrix least-

squares on F^2 using SHELXL-2018/3 (Sheldrick, 1996; 1997; 2015). The hydrogen atoms were freely refined. Graphics were drawn using DIAMOND (Putz and Brandenburg).

*Single-crystal X-ray data for **1***: $C_{11}H_{14}O_4$, M = 210.22, crystal size 0.28 x 0.22 x 0.18 mm^3, triclinic, space group P-1, a = 7.2824(5) Å, b = 8.3992(5) Å, c =9.1212(6) Å, V = 3349(4) $Å^3$, Z = 4, α = 100.645 (18) °, β = 105.6283 (18) °, γ = 103.0011 (18)° ρ (calcd) = 1.382 Mgm^{-3}, F(000) = 224, reflections collected/independent reflections 15249/2840 [R (int) =0.0248], final R indices [$I > 2s$ (I)] R_1 = 0.0355, wR_2 = 0.0924, goodness of fit on F^2 = 1.079. Crystallographic data for **1** have been deposited with the Cambridge Crystallographic Data Center (CCDC 1913728). These data can be obtained free of charge from the Cambridge Crystallographic Data Centre via http://www.ccdc.cam.ac.uk/data_request/cif.

Conflict of interest

The authors declare no conflict of interest.

Acknowledgement

The Alexander von Humboldt Foundation (APGM), the Ministry of Science, Research and Technology (MSRT) of Iran (AN) and the Iranian Mycological Society (AN) are gratefully acknowledged for fellowship support and research grants. We also thank Christel Kakoschke, Sabrina Karwehl and Wera Collisi for recording spectra and expert technical assistance, respectively.

References

Bills, G. F., Gloer, J. B., An Z. 2013. Coprophilous fungi: antibiotic discovery and functions in an underexplored arena of microbial defensive mutualism. Curr Opin Microbiol. 16, 549–565.

Bills, G. F., Gloer, J. B. 2016. Biologically active secondary metabolites from the fungi. Microbiol Spectr. 4.

Cheng, T., Chepkirui, C., Decock, C., Matasyoh, J. C., Stadler, M. 2019. Sesquiterpenes from an eastern African medicinal mushroom belonging to the genus *Sanghuangporus*. J. Nat. Prod. *in press*.

Chomcheon, P., Wiyakrutta, S., Sriubolmas, N., Ngamrojanavanich, N., Mahidol, C., Ruchirawat, S., Kittakoop, P. 2009. Metabolites from the endophytic mitosporic *Dothideomycete* sp. LRUB20. Phytochemistry. 70, 121–127.

Fujimoto, H., Satoh, Y., Nakayama, M., Takayama, T., Yamazaki, M. 1995. Four new immunosuppressive components, kobiin and kobifuranones A, B, and C, from an ascomycete, *Gelasinospora kobi*. Chem. Pharm. Bull. 46, 211–216.

Fujimoto, H., Satoh, Y., Yamazaki, M. 1998. Isolation of some immunosuppressive components from an Ascomycete, *Gelasinospora multiforis*. Chem. Pharm. Bull. 43, 547–552.

Fujimoto, H., Megumi, S, Nagano, J., Natori, H., Okuyama, E., Yamazaki, M. 1999. Immunomodulatory constituents from three ascomycetes, *Gelasinospora heterospora*, *G. multiforis*, and *G. longispora*. Chem. Pharm. Bull. 47, 71–76.

Fujimoto, H., Asai, T., Kim, Y.-P., Ishibashi, M. 2006. Nine constituents including six xanthone-related compounds isolated from two Ascomycetes, *Gelasinospora santi-florii* and *Emericella quadrilineata*, found in a screening study focused on immunomodulatory activity. Chem. Pharm. Bull. 54, 550–553.

Fujimoto, H. 2018. Immunomodulatory constituents from ascomycetous fungi. J. Nat. Med. 72, 20–31.

García, D., Stchigel, A. M., José, C. A., Guarro, J., Hawksworth, D. L. 2004. A synopsis and re-circumscription of *Neurospora* (syn. *Gelasinospora*) based on ultrastructural and 28S rDNA sequence data. Mycol. Res. 108, 1119–1142.

Helaly, S. E., Thongbai, B., Stadler, M. 2018. Diversity of biologically active secondary metabolites from endophytic and saprotrophic fungi of the ascomycete order Xylariales. Nat. Prod. Rep. 35, 992–1014.

Jayatilake, G. S., Thornton, M. P., Leonard, A. C., Grimwade, J. E., Baker, B. J. Metabolites from an antarctic sponge-associated bacterium, *Pseudomonas aeruginosa*.1996. J. Nat. Prod. 59, 293–296.

Karwehl, S., Stadler, M. 2016. Exploitation of fungal biodiversity for discovery of novel antibiotics. Curr. Topics Microbiol. Immunol. 398: 303–338.

Kim, G. S., Ko, W., Kim, J. W., Jeong, M.-H., Ko, S. K., Hur, J. S., Oh, H., Jang, J.-H., Ahn, J. H. 2018. Bioactive α-pyrone derivatives from the endolichenic fungus *Dothideomycetes* sp. EL003334. J. Nat. Prod. 81, 1084–1088.

Kuephadungphan, W., Macabeo, A. P.G., Luangsa-ard, J. J., Tasanathai K., Thanakitpipattana, D., Phongpaichit, S., Yuyama, K., Stadler, M. 2019. Studies on the biologically active secondary metabolites of the new spider parasitic fungus *Gibellula gamsii*. Mycol. Prog. 18, 135–146.

Machida, K., Matsuoka, E., Kasahara, T., Kikuchi, M. 2005. Studies on the constituents of *Juglans* species. I. Structural determination of (4*S*)- and (4*R*)-4-hydroxy-α-tetralone derivatives from the fruit of *Juglans mandshurica* MAXIM. var. *sieboldiana* MAKINO. Chem. Pharm. Bull. 53, 934–937.

Narmani, A., Teponno, R. B., Arzanlou, M., Babai-Ahari, A., Stadler, M. 2018. New secondary metabolites produced by the phytopathogenic fungus *Wilsonomyces carpophilus*. Phytochem. Lett. 26, 212–217.

Narmani, A., Teponno, R. B., Arzanlou, M., Surup, F., Helaly, S. E., Wittstein, K., Praditya, D. F., Babai-Ahari, A., Steinmann, E., Stadler, M. 2019. Cytotoxic, antimicrobial and antiviral secondary metabolites produced by the plant pathogenic fungus *Cytospora* sp. CCTU A309. Fitoterapia. 134, 314–322.

Phukhamsakda, C., Macabeo, A. P. G., Yuyama, K., Hyde, K., Stadler, M. 2018. Biofilm Inhibitory Abscisic Acid Derivatives from the Plant-Associated Dothideomycete Fungus, *Roussoella* sp. Molecules. 23, 2190–2095.

Zhao, J., Mou, Y., Shan, T., Li, Y., Zhou, L., Wang, M., Wang, J. 2010. Antimicrobial metabolites from the endophytic fungus *Pichia guilliermondii* isolated from *Paris polyphylla* var. *yunnanensis*. Molecules. 15, 7961–7970.

Zhao, Z., Zhao, K., Chen, H., Bai, X., Zhang, L., Liu, J. 2018. Terpenoids from the mushroom-associated fungus *Montagnula donacina*. Phytochemistry. 147, 21–29.

Sheldrick GM. SADABS, Software for empirical absorption correction; University of Gottingen: Germany, 1996.

Sheldrick, G. M. 2015. Crystal structure refinement with SHELXL. Acta Cryst. C71, 3–8.

Sheldrick, G. M. SHELXTL, Structure determination software programs; Bruker Analytical X-ray System Inc.: Madison, WI, 1997.

Diamond - Crystal and Molecular Structure Visualization Crystal Impact - H. Putz , K. Brandenburg GbR, Kreuzherrenstr. 102, 53227 Bonn, Germany.

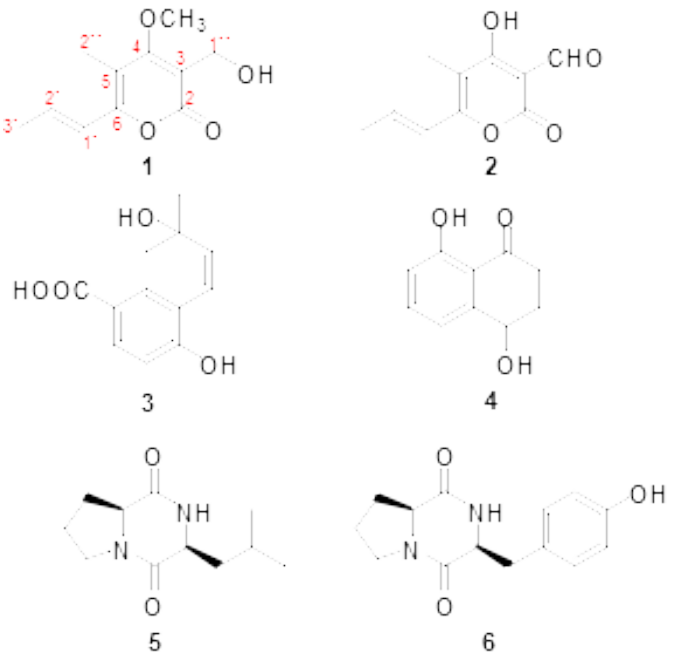

Fig. 1. Structures of secondary metabolites isolated from *Neurospora udagawae*.

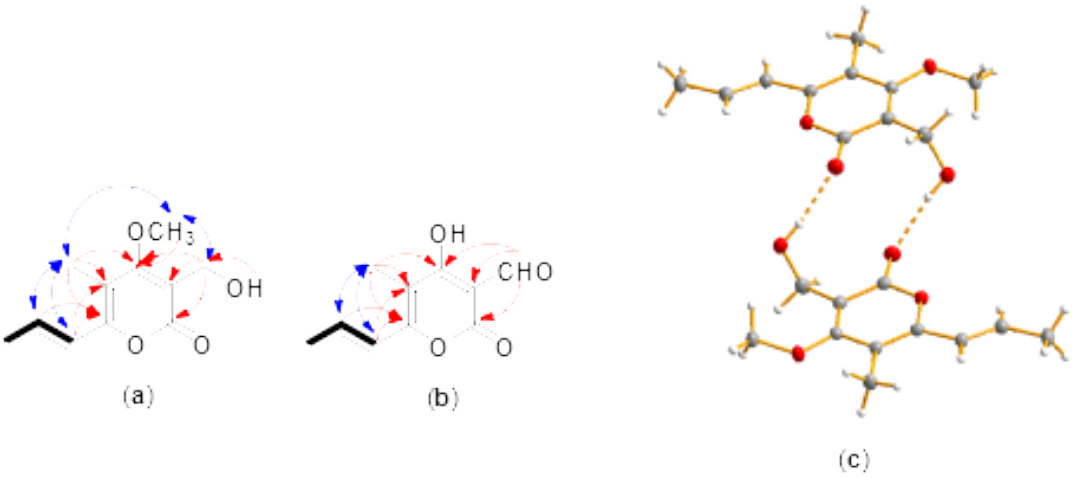

Fig. 2. COSY (bold lines), HMBC (red arrows) and ROESY (blue arrows) correlations in udagawanones A, **1** (a) and B, **2** (b), and H-bonded dimeric single-crystal X-ray structure (c) of **1**.

Table 1

^{1}H and ^{13}C NMR data for udagawanones A (**1**) $CDCl_3$[a] and B (**2**) in MeOH-d_4[b].

	1		**2**	
Position	δ_H (ppm)	δ_C (ppm)	δ_H (ppm)	δ_C (ppm)
2	-	165.1	-	163.8
3	-	111.3	-	105.4
4	-	169.4	-	166.0
5	-	108.6	-	96.4
6	-	154.2	-	158.4
1`	6.25, dq (15.3, 1.7)	119.9	6.54, dq (15.2, 1.6)	121.8
2`	6.69, dq (15.4, 7.0)	135.0	6.82, dq (15.2, 6.9)	139.5
3`	1.91, dd (7.0, 1.7)	9.4	1.98, dd (6.9, 1.6)	9.4
1``	4.56, s	61.9	9.94, s	191.8
2``	1.96, s	18.7	2.03, s	19.0
4-OMe	3.96, s	55.8	-	-
1`-OH	3.05, br s	-	-	-

[a] ^{1}H and ^{13}C NMR spectra were recorded at 500 and 125 MHz, respectively.

[b] ^{1}H and ^{13}C NMR spectra were recorded at 700 and 175 MHz, respectively.